Trees (2016) 30:609–625
DOI 10.1007/s00468-015-1304-2

ORIGINAL ARTICLE

Study of tension wood in the artificially inclined seedlings of *Koelreuteria henryi* Dummer and its biomechanical function of negative gravitropism

Li-Fen Hung[1] · Ching-Chu Tsai[1] · Shiang-Jiuun Chen[1] · Yan-San Huang[2] · Ling-Long Kuo-Huang[1]

Received: 23 April 2015 / Revised: 23 September 2015 / Accepted: 25 September 2015 / Published online: 6 October 2015

Abstract

Key message **Stem reorientation is critical to tree survival. With anatomical observation and strain measurement, the tension wood formation and biomechanical behavior were studied to gain insights into tree uprighting process.**

Abstract Tension wood plays a role in maintaining the mechanical stability of angiosperm trees. Both biological and physical aspects of tension wood are essential in understanding the mechanism of trunk or branch reorientation. In this study, we worked on both tension wood formation and its biomechanical function in artificially inclined 2-year-old *Koelreuteria henryi* seedlings. The tension wood formation and reorientation process of the trunk last for about 3 months. With pinning method, we confirmed that at the beginning of inclination the cambial zone including the vascular cambium and the developing normal wood fibers on the upper side of the inclined trunk perceives the onset of mechanical change and starts to produce G-fibers that generate a strong contractile released growth strain (RGS) for gravitropic correction. Stronger contractile RGS and more tension wood were found at the trunk base than at the half-height, suggesting that the trunk base plays a key role in trunk uprighting of *K. henryi* seedlings. The eccentric cambial growth in the tension wood side increases the efficiency of gravitropic correction and the compressive strains measured in the opposite wood of some inclined seedlings also help the upright movement.

Keywords *Koelreuteria henryi* Dummer · Tension wood · G-fibers · Gravitropic correction · Bending dynamics

Communicated by Y. Sano.

✉ Ling-Long Kuo-Huang
linglong@ntu.edu.tw

[1] Institute of Ecology and Evolutional Biology, National Taiwan University, 1, Roosevelt Rd. Sec. 4, Taipei 106, Taiwan

[2] Department of Forestry, National Chung Hsing University, 205, Kuo Kuang Rd., Taichung 402, Taiwan

Introduction

Trees keep the mechanical stability by adjusting the position of their trunk and branches in response to various environmental disturbances and gravitational stimulus (Ewart and Mason-Jones 1906; Fisher and Stevenson 1981; Gardiner et al. 2014; Sinnott 1952; Wilson and Archer 1979). Leaning tree trunks and branches could reorient to an equilibrium position by producing reaction wood accompanying increased cambial growth. In gymnosperms, compressive growth stress induced by compression wood is generated on the lower side to push the leaning trunk and branches upward. However, in angiosperms, tension wood generally develops on the upper side and produces tensile stress to pull the leaning trunk or branches upward (Onaka 1949; Scurfield 1973; Sinnott 1952; Wilson and Archer 1977).

Compression wood in gymnosperms is composed of tracheids which are round in cross section and possess a thicker secondary wall with greater MFA and higher lignin content than those in normal wood (Wardrop and Dadswell 1950). Typical tension wood is featured by the gelatinous fibers (G-fibers) with the S2 and/or S3 layers replaced by a special gelatinous layer (G-layer) which consists of highly crystalline cellulose fibrils that are almost parallel to the fiber axis (Scurfield 1973; Wardrop and Dadswell 1948).

Nevertheless, not all angiosperms produce typical tension wood with G-fibers. Onaka (1949) found that 79 % of 346 angiosperms produce G-fibers; Höster and Liese (1966) examined 266 trees and shrubs and found only ca. 50 % of the investigated species exhibit G-fibers in branch wood and ca. 25 % in root wood. Fisher and Stevenson (1981) detected G-fibers on the upper side of the branches in 46 % of 122 dicotyledonous species in 46 families. Besides, *Buxus microphylla* var. *insularis* Nakai, even produces compression wood on the lower side of the leaning trunks, exemplifying the considerable diversified reaction anatomy in angiosperms (Yoshizawa et al. 1993a, b).

Among species producing G-fibers, there are variations existing in their cell wall structure. The cell wall of a normal wood fiber is composed of a primary wall (P) and a secondary wall consisting S1, S2, and/or S3. G-fibers may contain cell walls consisting P+S1+G, P+S1+S2+G, or P+S1+S2+S3+G (Scurfield 1973; Wardrop and Dadswell 1955). Besides, a special polylaminate secondary wall structure with an alternate of lightly lignified thick layers and more lignified thin layers was found in tension wood of *Casearia javitensis* (Clair et al. 2006c) and *Laetia procera* (Poepp.) Eichl (Ruelle et al. 2007b) in Flacourtiaceae family.

The presence of G-fibers on the upper side of the inclined stem is correlated with high tensile growth strains or stresses (Fang et al. 2007; Ruelle et al. 2011; Washusen et al. 2003a). The mechanism of stress generation is related to the features of G-fibers including small MFA (Donaldson 2008; Okuyama et al. 1994), increased cellulose lattice spacing (Clair et al. 2006b, 2011) and high content of xyloglucan (Baba et al. 2009; Mellerowicz and Gorshkova 2012; Mellerowicz et al. 2008; Nishikubo et al. 2011). Besides, the magnitude of growth stress is influenced by the thickness of G-layer and the ratio of G-fiber area (Fang et al. 2008).

To explain the mechanism of upward bending process, Fournier et al. (1994a) presented a simple biomechanical model according to the maturation strain asymmetry of a leaning trunk. Coutand et al. (2007) applied the model to investigate the gravitropic response of poplar trunks and found it limited to explain the total variance. For providing the theoretical predictions on biomechanical design and long-term stability of trees, Alméras and Fournier (2009) expanded the original model with the gravitational disturbance, eccentric growth, and heterogeneous stiffness. Based on Fournier's original model, Huang et al. (2010) developed an equivalent model using spring-back strain (SBS) to evaluate self-weight bending moment and made the model practical and easy to follow. Huang's model has been successfully applied in the prediction of bending dynamics of broadleaf tree branches (Tsai et al. 2012).

Koelreuteria henryi Dummer (synonym: *K. elegans* ssp. *formosana*) in Sapindaceae family is a deciduous tropical tree species with meandering branches. It is endemic to Taiwan but is listed as an invasive species in south-east Queensland, Australia (Batianoff and Butler 2002) and in Florida, USA by Florida Exotic Pest Plant Council. The findings of unusual eccentric growth and released growth strain (RGS) distribution in its branches (unpublished data) have led us to conduct studies for having a comprehensive insights into the role of reaction wood formation in the leaning trunk and branches during the tree form adjustment. In this paper, we monitored the reorientation process of the artificially inclined trunks of *K. henryi* seedlings. The growth strain distribution and related eccentric growth were surveyed. Besides, we used the pinning method to directly identify the onset of G-fiber formation. The cell wall structure and distribution of G-fibers were also investigated. Finally, Huang's model (Huang et al. 2010) was applied for analyzing the bending dynamics of the inclined trunks.

Materials and methods

Seedlings and experimental design

To study the trunk reorientation process of *Koelreuteria henryi* seedlings, two greenhouse experiments were conducted. On Feb 18 2009, twenty-four 2-year-old seedlings germinated from seeds were purchased from a nursery in Changhua (central Taiwan). The naturally defoliated seedlings were transplanted in a 5-l pot with Yang-Ming-Shan soil, perlite, vermiculite, and peat moss (1:1:1:1) and acclimated in the greenhouse of National Taiwan University (25°00′N, 121°27′E). On April 23, the average height of seedlings was 82.9 ± 18.8 cm and the average basal diameter was 8.44 ± 0.94 mm. Twelve seedlings (T1 ~ T12) were randomly selected and artificially inclined at an angle of about 30° (28.8 ± 2.7°) from vertical by placing the pots on fixed PVC pipes (Fig. 1a) and the other 12 seedlings (C1 ~ C12) were kept upright as controls. The trunk base (at 10 cm above the soil) and the half-height of all seedlings were pre-marked with white-out for subsequent RGS measurement. The bark of each seedling at 1 cm below the measuring site was pinned by an insect needle (0.4 mm in diameter) on the upper and the lower sides of the inclined seedlings and the corresponding A and B sides of the control seedlings. By pinning, the cambial zone was wound and triangular callus tissue was formed and thus marked the location of vascular cambium at the pinning time (Yoshimura et al. 1981). We monitored the uprighting process of the inclined seedlings. Seasonally, we measured RGSs of the seedlings and investigated the

related anatomical structures. We also applied Huang's model (Huang et al. 2010) to analyze the bending dynamics.

On April 25, 2012 we started a similar experiment with monthly sampling for 3 months. The nine studied seedlings (C13 ~ C15 for control and T13 ~ T18 for inclination) were obtained through pruning the stems of the seedlings above the soil in 2011 and left one epicormic shoot to become the main stem. The average height was 103.2 ± 12.6 cm and the average basal diameter was 9.54 ± 0.92 mm. One control and two inclined seedlings were sampled monthly for measuring RGSs and examining the tension wood formation and then predict the bending tendency.

Dynamics of uprighting process

To monitor the angle change, pictures of each inclined seedling of the 2009 experiment were taken with a digital camera (Nikon D3) weekly for the first season, biweekly for the second season, and monthly for the third and fourth seasons (Fig. 1b). Photographs of each seedling were assembled with Photoshop CS5 to examine the trunk shape evolution during the uprighting process. Because the radius of curvature is generally large in the inclined trunk of *K. henryi* seedlings, the proximal angle (θ) (Fig. 1b) of each seedling was measured from the pictures using Image J and was then used to analyze the uprighting process.

Released growth strain (RGS) measurement

Released growth strain was measured seasonally (7/23, 10/20 in 2009 and 1/28, 4/21 in 2010) in the 2009 experiments and monthly (5/25, 6/25, 7/25) in the 2012 experiment. To measure RGS, the bark of the marked measuring site was removed. The strain gauge (FLA-5-11-5LT, Tokyo Sokki Kenkyujo Co., Ltd) was glued to the surface of secondary xylem using cyanoacrylate adhesive (Tokyo Sokki Kenkyujo Co., Ltd) and connected to a data logger (TD 102, Tokyo Sokki Kenkyujo Co., Ltd) (Fig. 1c). After the gauge being zeroed, the seedling was firstly cut at the trunk base and held straight to read spring-back strain (SBS). Then, RGS was measured after the cross-cutting at the positions 3 mm apart from the upper and the lower rims of the gauge (Huang et al. 2010).

Wood anatomical structure and morphometry

Stem segments of 3 cm long with the marked pinholes were fixed and stored in FPGA (Formalin:Propionic acid:Glycerol:95 % Alcohol:distilled water = 1:1:3:7:8). Using sliding microtome (ERMA optical works, Ltd), 20 μm thick wood sections containing pinning-induced callus were collected and stained with 1 % toluidine blue O in 1 % sodium borax (TBO) or double stained with 0.5 % safranin O and 0.1 % alcian blue (in 0.3 % acetic acid). Besides, for cellulose test some wood sections were

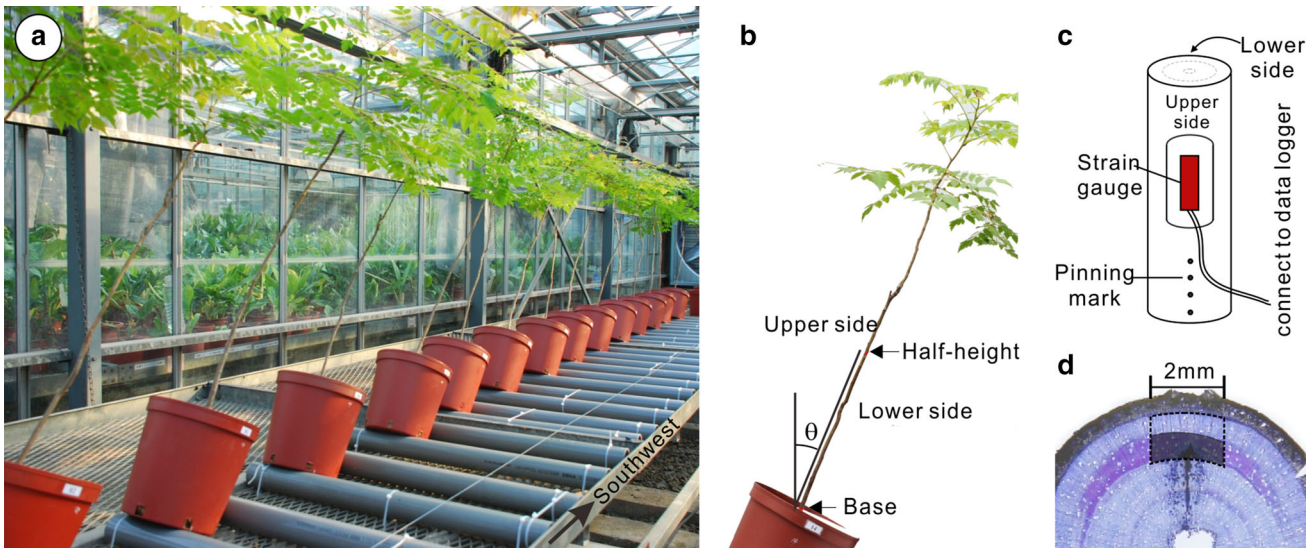

Fig. 1 Experimental design and sampling methods for studying reaction wood formation in inclined *Koelreuteria henryi* seedlings. **a** Photograph of the inclined seedlings at the beginning of inclination. The experiment was conducted in the green house and each pot was placed on a pair of fixed PVC pipes to set the tilting angle. **b** The picture showing the RGS measuring sites (the base and the half-height of the trunk) and the positions (the upper and the lower sides of the inclined trunk). Pictures of each inclined seedling were taken weekly to monthly and from which the proximal angles (θ) (the angle of the line joining the trunk base and the half-height to the vertical) were measured. **c** Illustration of the locations of pinning marks and RGS measurement. **d** Illustration of tension wood ratio measurement: dotted line outlining the measured whole wood area and grey area marking the area of tension wood

histochemically stained with zinc chloride-iodine. G-layers were stained purple-red with zinc chloride-iodine, purple with TBO, and light blue with alcian blue.

Whole stem sections were collected and photographed using a digital camera (Sony DSC-T200). The vertical and horizontal diameters were measured with Image J and then the average radius (R) was calculated. The area of tension wood formed after inclination by each inclined seedling was also measured on the cross section using image J. The ratio of tension wood on the upper side (hereafter tension wood ratio) was calculated as tension wood area over whole wood area formed after inclination. Concerned the effective regions of the strain gauge measurement, we confined the whole wood area as 2 mm in width and between the pinning-induced callus and the recently matured wood (Fig. 1d). To measure the wood growth increment in the trunks, the upper and the lower sides of the trunk sections containing cambial marks and new formed wood tissue were photographed by Nikon D3 on Leica Diaplan Light Microscope. The variation of radius, i.e. the growth increments during the period of experiment including ΔR_a and ΔR_b for the A side and the B side of the control seedling; ΔR_u and ΔR_l for the upper side and the lower side of the inclined seedling were measured from the margin of the cambial mark to the cambial zone with Image J. The average growth increment (ΔR) was then calculated, ΔR is equal to $(\Delta R_a + \Delta R_b)/2$ for the control seedling and $(\Delta R_u + \Delta R_l)/2$ for the inclined seedling.

For studying the cambial activity and the cell wall ultrastructure, stem blocks were cut from 20 cm above the soil. The wood samples ($1 \times 1 \times 2$ mm^3) of the upper and the lower sides were doubly fixed with 2.5 % glutaraldehyde (in 0.1 M phosphate buffer) followed by 1 % osmium tetroxide (in 0.1 M phosphate buffer), dehydrated with acetone series. For TEM, the samples were infiltrated and embedded in Spurr's resin (Spurr 1969) and cut using an ultramicrotome (Ultracut E). Semi-thin sections (1 μm) were stained with TBO and photographed by Nikon D3 under Leica Diaplan Microscope. Ultra-thin sections were stained with a fresh mixture of 5 % UA and 1 % KMnO4 (1:3) and observed with Hitachi H-7650. For SEM, the samples were further dehydrated by critical point drying method (Hitachi HCP-2) and coated with gold (Hitachi E101) and observed by FEI Inspect S. The MFA was measured from the SEM photographs using Image J.

Prediction of the bending dynamics of trunks

The bending dynamics was predicted by Huang's biomechanical model (Huang et al. 2010). In the model, the rate of change in curvature associated with the wood growth increment (dC/dR) is expressed as

$$\frac{dC}{dR} = \frac{dC_s + dC_g}{dR} = \frac{4(\beta - \alpha)}{R^2} \quad (1)$$

where dC_s/dR ($=4\beta/R^2$) is the rate of change in curvature due to spring-back (self-weight) associated with growth increment, and dC_g/dR ($=-4\alpha/R^2$) is due to asymmetric growth strain; spring-back strain parameter (β) associated with gravitational force is defined as half the difference of the SBS between the upper and lower sides: $\beta = (\varepsilon_{su} - \varepsilon_{sl})/2$; released growth strain parameter (α) associated with gravitropic correction is defined as half the difference of the RGS between the upper and the lower side: $\alpha = (\varepsilon_{gu} - \varepsilon_{gl})/2$. When dC/dR is positive, the branch tends to bend upward; when it is negative, the branch tends to bend downward. Equation (1) can be further corrected for eccentric radial growth by substituting α with $\alpha' = [\varepsilon_{gu}(dR_u/dR) - \varepsilon_{gl}(dR_l/dR)]/2$, where dR_u is wood growth increment of the upper side and dR_l the lower side. The dR_u/dR and dR_l/dR were estimated with the measured $\Delta R_u/\Delta R$ and $\Delta R_l/\Delta R$, respectively. The corrected rate of change in curvature is expressed as dC'/dR.

Statistics

All data were tested for normality by Shapiro–Wilk test. When the data conformed to normal distribution, the mean values of RGSs of the upper and the lower sides were compared with paired t test, for which t value and p value were provided. The mean values among different inclination durations (3, 6, 9 and 12 months) were compared with one-way ANOVA, for which F value and p value were provided. For heteroscedastic data or data deviated from normal distribution, Kruskal–Wallis rank sum test was used instead, for which *Chi* square and p value were provided. Either ordinary linear regression or polynomial regression was used to analyze the relationship between strain magnitude and inclination duration, and between RGSs and tension wood ratio, for which, r^2 and p value were provided. Statistical tests were performed using Origin (OriginalLab, Northampton, MA) and R version 3.1.1 (the R Core Team 2013). All statistical relationships were considered to be significant at $p < 0.05$.

Results

Dynamics of the uprighting process of the inclined seedlings

In the 2009 experiment, we found that the uprighting process occurred mainly in the first 3 months after inclination in spring season. One week after tilting, five out of the 12 inclined seedlings sagged a little, while others

showed only little change in orientation (Fig. 2a). Two weeks after tilting, all the 12 inclined seedlings curved upward. The proximal angle change after inclination was 2.7° (SD = 1.6°, $n = 12$) in the first month, 2.7° (0.8°) in the second month, and 2.1° (1.0°) in the third month; i.e., the total proximal angle change was 7.5° (SD = 2.52°, $n = 12$) in the first season. Thereafter, the uprighting process was much slower: the proximal angle changed 1.5° (SD = 1.2°, $n = 9$) in the second season, 2.2° (1.1°, $n = 6$) in the third season, and 1.5° (0.9°, $n = 3$) in the fourth season (Fig. 2a). At the end of this experiment, the average tilting angle for the last three seedlings was 19.9 ± 3.7°. The apical region of the seedlings curved up soon after the inclination, they were straight and vertical

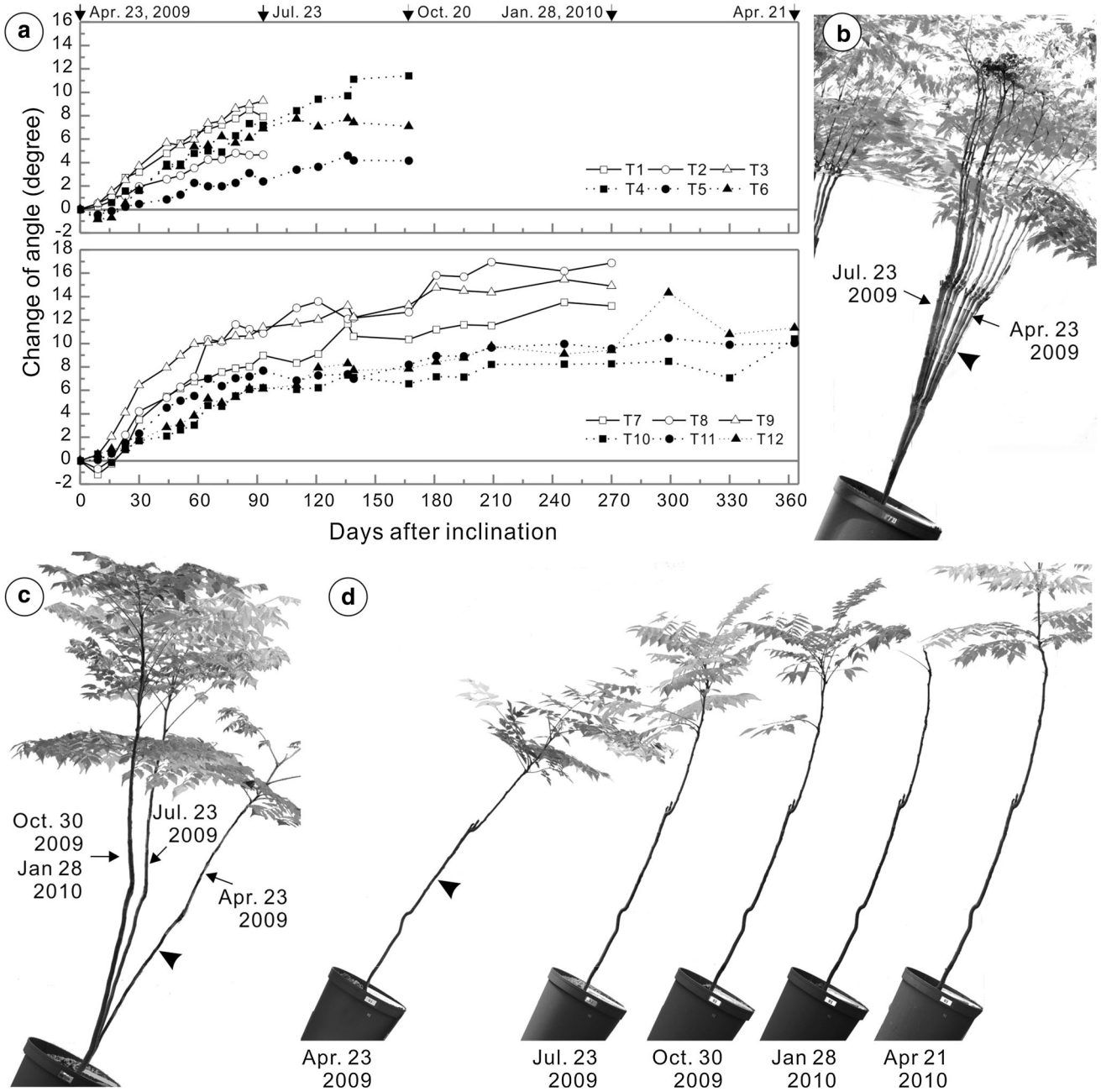

Fig. 2 **a** Changes of the proximal angle of the inclined seedlings in the 2009 experiment, positive for uprighting and negative for sagging. **b** Tree shapes of the T3 seedling from April 23 to July 23, 2009. The proximal angle changed from 25.1° to 15.8° in these 3 months. **c** Seasonal tree shapes of the T9 seedling (April, July, October 2009 and January 2010). The tree shapes on the last two seasons were similar; however, fewer leaves were observed on January 2010. **d** Seasonal photos of the T10 seedling (April, July, October 2009 and January, April 2010). *Arrow heads* point out the half-height of the trunks

after 6- to 8-weeks and mostly stayed vertical and only some of them showed overcorrection (Fig. 2).

Released growth strain distribution

Since the stress is proportional to the strain within a proportional limit (Archer 1986), we estimated the pre-stress by measuring the RGSs of green wood. Figure 3a, b shows that the control seedlings exhibited either contractive (−) or extensive (+) strains on both sides of the trunk base and the half-height (Fig. 3; Table 1). In the 2009 experiment, the RGSs measured on the A and B sides of the control seedlings showed no significant difference ($t = -0.343$, $p = 0.735$), indicating that in the green house there was no perspective effect. The average RGSs were small: −120.21 με at the trunk base and −76.67 με at the half-height, while strain values were more stable at the trunk base (SD = 145.19) than at the half-height (SD = 232.48) ($F = 0.379$, $p = 0.012$), because two stronger contractive values (−610 and −652 με) were measured at the half-height on the last sampling date. The RGSs of the trunk base of the control seedlings in the 2012 experiment fell into the range of those in the 2009 experiment (Fig. 3b).

In the 2009 experiment, the inclined seedlings exhibited only contractive strains on the upper sides (ε_{gu}: −1690 to −64 με), while on the lower side either contractive or extensive strains were measured at both the trunk base and the half-height (ε_{gl}: −1276 to +495με) (Fig. 3c, d; Table 1). The ε_{gu} and ε_{gl} showed no significant change during the whole experiment period (ε_{gu}: $\chi^2 = 3.43$, $p = 0.329$ for the trunk base, $\chi^2 = 2.897$, $p = 0.408$ for the half-height; ε_{gl}: $\chi^2 = 1.256$, $p = 0.740$ for the trunk base, $\chi^2 = 1.051$, $p = 0.789$ for the half-height), whereas the value of ε_{gu} was significantly smaller than ε_{gl} (paired $t = -2.653$, $p = 0.011$ for the trunk base, $t = -2.956$, $p = 0.007$ for the half-height). Similar results were

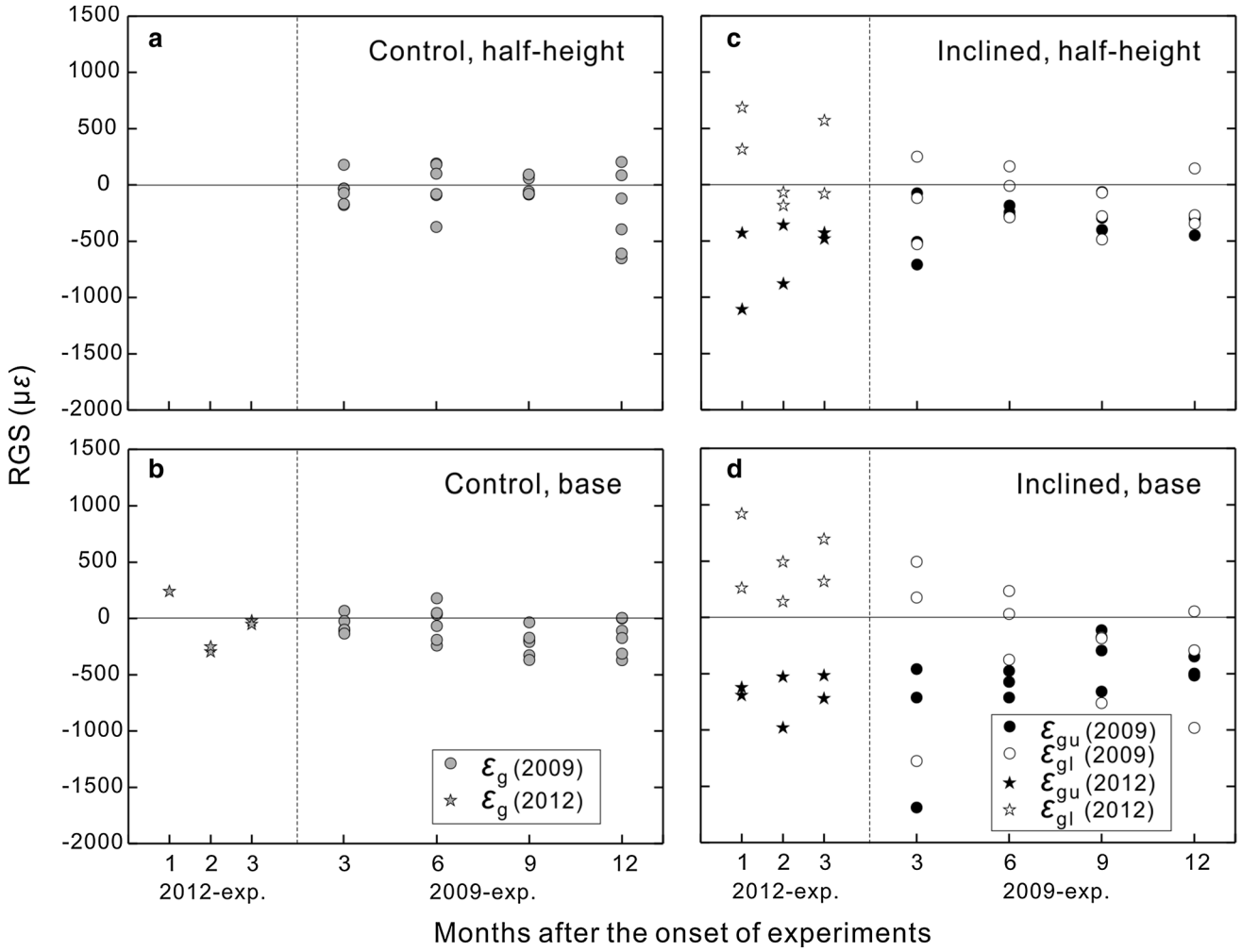

Fig. 3 RGS distribution at the half-height (**a**, **c**) and the trunk base (**b**, **d**) of the control (**a**, **b**) and inclined (**c**, **d**) *K. henryi* seedlings in the 2009 and 2012 experiment. ε_g RGS of both A side (ε_{ga}) and B side (ε_{gb}) for the control seedlings, ε_{gu} and ε_{gl}, RGS for the upper and the lower side of inclined seedlings

Table 1 Measured data of the control and the inclined seedlings of *Koelreuteria henryi*

Growth duration	Measuring site	R (mm)	ΔR_a (mm)	ΔR_b (mm)	ΔR (mm)	RGS (με)		Measuring site	R (mm)	ΔR_u (mm)	ΔR_l (mm)	ΔR (mm)	TW_{area} (mm^2)	SBS (με)		RGS (με)	
						ε_{ga}	ε_{gb}							ε_{su}	ε_{sl}	ε_{gu}	ε_{gl}
2009 experiment																	
3 months	C1b	3.6	0.34	0.34	0.34	69	−22	T1b	4.02	1.36	0.38	0.87	8.4	−261	401	−712	177
	C1h	3.1	0.36	0.25	0.31	−32	−32	T1h	3.60	1.07	0.34	0.71	5.92	−95	130	−710	−528
	C2b	4.1	0.51	0.54	0.53	−108	−100	T2b	5.03	1.36	0.62	0.99	10.81	–	–	−1690	−1276
	C2h	3.7	0.37	0.61	0.49	180	−71	T2h	4.10	0.70	0.62	0.66	2.89	–	–	−507	−118
	C3b	4.6	0.68	0.55	0.62	−100	−133	T3b	4.17	1.00	0.21	0.61	9.71	–	–	−458	495
	C3h	3.8	0.63	0.46	0.55	−177	−169	T3h	3.46	0.71	0.13	0.42	2.54	–	–	−77	248
6 months	C4b	4.8	1.01	1.13	1.07	35	49	T4b	4.92	1.89	0.78	1.34	10.65	−165	130	−573	−375
	C4h	3.8	0.87	0.78	0.83	191	−81	T4h	3.96	1.19	0.71	0.95	4.71	−65	119	−273	−290
	C5b	5.0	1.18	1.06	1.12	−240	−66	T5b	6.15	2.16	1.29	1.73	6.6	−350	404	−476	235
	C5h	4.0	0.9	0.82	0.86	−372	181	T5h	4.09	1.29	1.07	1.18	4.52	−96	127	−186	−10
	C6b	5.1	1.35	1.76	1.56	−190	180	T6b	5.20	2.31	1.02	1.67	9.24	−240	237	−712	30
	C6h	4.3	1.59	1.24	1.42	−90	100	T6h	3.95	1.51	0.57	1.04	3.64	−116	173	−246	162
9 months	C7b	5.5	1.63	1.07	1.35	−35	−369	T7b	5.41	2.62	1.89	2.26	7.93	12	78	−295	−176
	C7h	4.4	1.19	0.72	0.96	85	−85	T7h	4.38	1.53	1.38	1.46	2.19	64	−36	−64	−72
	C8b	4.9	1.49	1.56	1.53	−191	−209	T8b	5.52	3.49	0.94	2.22	22.1	−48	108	−659	−760
	C8h	4.0	1.11	1.19	1.15	−58	−78	T8h	4.35	1.85	1.61	1.73	5.01	42	27	−294	−281
	C9b	4.6	0.93	1.36	1.15	−326	−171	T9b	5.09	2.37	1.23	1.80	9.07	−24	27	−114	−186
	C9h	4.0	0.96	1.02	0.99	59	93	T9h	4.04	1.60	1.37	1.49	3.94	60	−25	−400	−486
12 months	C10b	6.0	1.46	1.16	1.31	−108	−312	T10b	5.04	1.86	0.83	1.35	7.58	−140	−348	−348	55
	C10h	5.0	1.38	1.15	1.27	−394	−610	T10h	3.99	1.26	0.43	0.85	5.22	−46	−58	−278	144
	C11b	5.9	1.52	1.31	1.42	0	6	T11b	5.27	2.36	0.70	1.53	10.38	−18	176	−516	−980
	C11h	4.7	0.97	0.92	0.95	87	205	T11h	3.62	1.09	0.49	0.79	3.33	21	74	−450	−272
	C12b	7.2	3.48	2.86	3.17	−371	−173	T12b	6.63	3.01	1.33	2.17	17.26	−106	56	−498	−291
	C12h	6.1	2.52	1.83	2.18	−652	−120	T12h	4.96	1.86	1.49	1.68	7.57	132	−169	−301	−345
2012 experiment																	
1 months	C13b	4.29	0.15	0.15	0.15	–	240	T13b	4.41	0.31	0.20	0.26	–	−576	1004	−624	919
								T13h	–	–	–	–	–	−763	825	−1108	686
								T14b	3.81	1.00	0.32	0.66	–	−315	470	−693	260
								T14h	–	–	–	–	–	−371	475	−430	315
2 months	C14b	4.52	0.37	0.39	0.38	−297	−252	T15b	4.66	1.07	0.35	0.71	–	−273	422	−528	139
								T15h	–	–	–	–	–	−150	254	−360	−70
								T16b	4.82	1.13	0.42	0.78	–	−680	812	−980	492
								T16h	–	–	–	–	–	−527	583	−882	−184

Table 1 continued

Growth duration	Measuring site	R (mm)	ΔR_a (mm)	ΔR_b (mm)	ΔR (mm)	RGS (με)		Measuring site	R (mm)	ΔR_u (mm)	ΔR_l (mm)	ΔR (mm)	TW_{area} (mm^2)	SBS (με)		RGS (με)	
						ε_{ga}	ε_{gb}							ε_{su}	ε_{sl}	ε_{gu}	ε_{gl}
3 months	C15b	3.6	1.08	1.15	1.12	−23	−52	T17b	4.92	1.42	0.74	1.08	–	−624	716	−721	318
								T17h	–	–	–	–	–	−182	363	−428	−81
								T18b	4.13	1.38	0.25	0.81	–	−340	681	−516	694
								T18h	–	–	–	–	–	−267	431	−481	570

C control seedling, *T* inclined seedling, *b* base, *h* half-height, *R* the average radius of wood calculated from the vertical and horizontal diameters, ΔR_a and ΔR_b growth increment on two opposite sides of the stem in control seedlings, ΔR_u and ΔR_l growth increment of the upper and the lower side of the stem in inclined seedlings, ΔR the average growth increment, *RGS* released growth strain, ε_{ga} and ε_{gb} released growth strain on the A and the B side of the trunk in control seedlings, ε_{gu} and ε_{gl} released growth strain on the upper and the lower side of the trunk in inclined seedlings, *SBS* spring-back strain, ε_{su} and ε_{sl} spring-back strain on the upper and the lower side of the stem in inclined seedlings, TW_{area} total area of tension wood formed after inclination, – not measured

observed in the 2012 experiment; however, the RGSs on the lower side are more extensive than those in the 2009 experiment (Fig. 3c, d). When the data of the two experiments were pooled, a negative relationship was found at the trunk base between ε_{gl} and inclination duration ($r^2 = 0.29$, $p = 0.022$); the correlation coefficient is improved when a potential outlier was removed ($r^2 = 0.59$, $p < 0.01$).

Eccentric growth and tension wood formation

Eccentric growth occurred in all inclined seedlings but not in the control seedlings (Fig. 4; Table 1). The control seedlings present no eccentric growth at either the trunk base or the half-height on all the sampling dates (Fig. 4a, b). For the inclined seedlings, the amount of wood growth increment on the lower side (ΔR_l) of the trunk was similar with that of the control seedlings (ΔR_a and ΔR_b) (Fig. 4; Table 1). However, the wood growth increment was larger on the upper side (ΔR_u) than on the lower side (ΔR_l) (Fig. 4c, d; Table 1). The paired *t*-test revealed significant (<0.05) or at least marginally significant ($0.05 < p < 0.1$) results.

All fibers including G-fibers, opposite and normal wood fibers in *K. henryi* were all living fibers generally containing massive starch grains (Fig. 5). The histochemical results suggested that lignin was deposited in all the cell wall layers except for the G-layer and the double staining with safranin O and alcian blue gave an excellent contrast for the cell wall layers of G-fibers (Fig. 5c, f). Ultrastructure study revealed that the secondary wall of the fibers in normal wood and opposite wood consisted of S1+S2+S3 (Fig. 6a, c) while that of the G-fibers consisted of S1 and an additional G-layer (Fig. 6b, d). The microfibril angle of S2 layer in the normal wood fiber of *K. henryi* was about 25° (Fig. 6e); however, the microfibrils in the G-layer were almost parallel to the axis of the G-fiber (Fig. 6f).

In the inclined *K. henryi* seedlings, a crescent tension wood zone containing G-fibers was observed on the upper side of the wood section (Fig. 7). Included in the tension wood zone, a triangular callus induced by pinning was observed. The lower rim of the callus marked the position of cambial zone at the onset of pinning (Fig. 7a, d). The induced G-fibers were mostly observed on the outer side of the marked cambial zone, but a few layers of G-fibers were detected on the inner side (Fig. 7a, d). Two out of the three inclined seedlings were still producing G-fibers on the upper side of the trunk after 3-months inclination when the cambium on the lower side appearing inactive (Fig. 8). No developing G-fibers were observed 6 months after inclination. For the control seedlings, no G-fibers were observed in the wood tissues formed after the experiment except on the B side of the half-height in the C10 seedling.

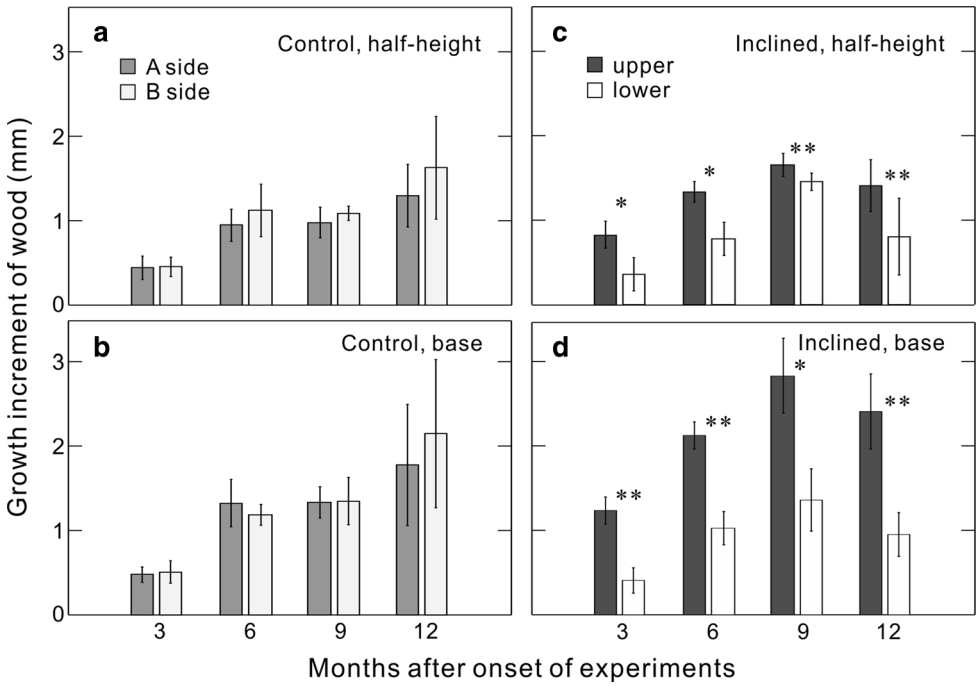

Fig. 4 Radial wood growth increments at the half-height (**a**, **c**) and the trunk base (**b**, **d**) of the control (**a**, **b**) and the inclined (**c**, **d**) *K. henryi* seedlings in the 2009 experiment. The *error bars* represent standard errors. $*0.05 < p < 0.1$, $**p < 0.05$ ($n = 3$)

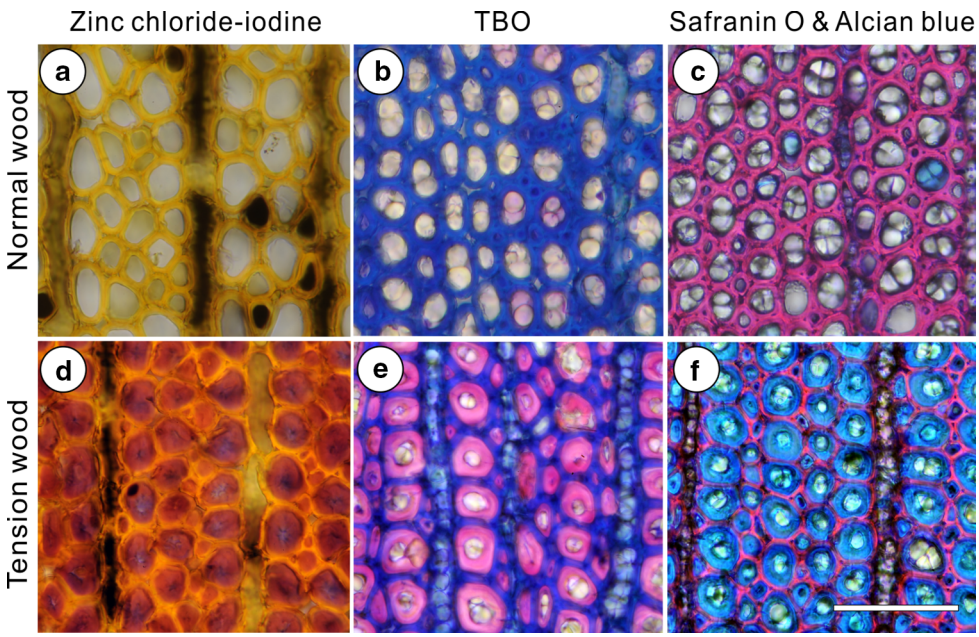

Fig. 5 Histochemical stainings for normal wood (**a**–**c**) and tension wood (**d**–**f**). G-layers were stained *purple-red* with zinc chloride-iodine (**d**); *purple* with TBO (**e**); and *light blue* with alcian blue (**f**). *Bar* 50 μm

The relationship between RGSs and tension wood ratio

In the 2009 experiment, tension wood containing G-fibers near the cambial zone (Fig. 8) together with large, negative ε_{gu} values (Table 1) were observed on the upper side of the inclined trunks 3 months after inclination. After 6-month inclination, near the cambial zone G-fibers were no longer found, and the magnitude of ε_{gu} was reduced but still larger than ε_{gl} (Table 1). Figure 9 shows that the magnitude of RGSs on the upper side increased as the tension wood ratio increased ($r^2 = 0.46$; $p < 0.01$). The correlation coefficient could be higher if the outlier was removed ($r^2 = 0.54$; $p < 0.01$).

Prediction of bending dynamics

For analyzing the bending dynamics, we pooled the data from the inclined seedlings of *K. henryi* in the 2009 and the 2012 experiments excluding those of the seedlings sampled

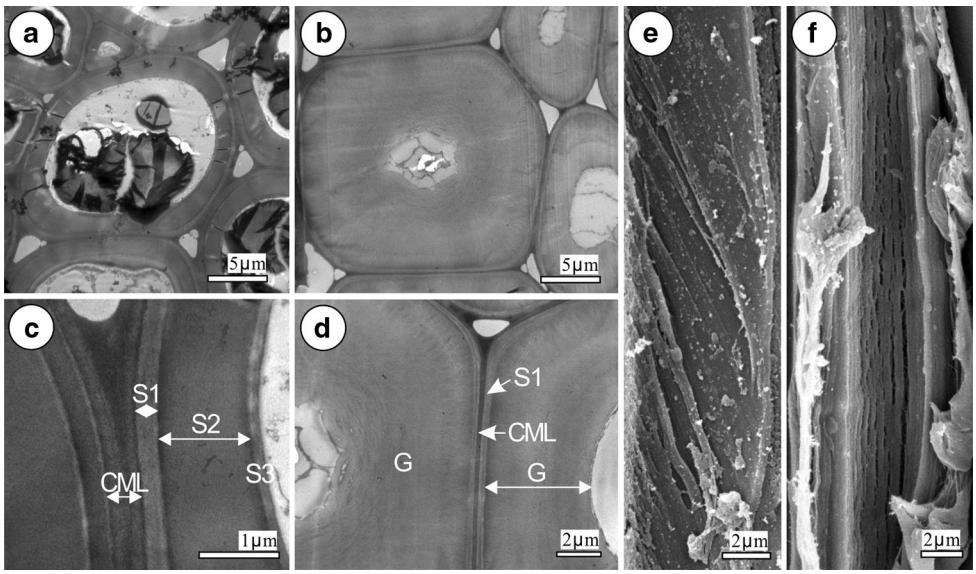

Fig. 6 TEM (**a**–**d**) and SEM (**e**, **f**) photographs of opposite wood fibers (**a**, **c**, **e**) and G-fibers (**b**, **d**, **f**). The secondary wall of the opposite wood fiber consisted of S1+S2+S3, while the secondary wall of the G-fiber was composed of S1+G. *S* secondary wall, *CML* compound middle lamella, *G* G-layer

9 and 12 months after inclination. Because the inclined seedlings recovered to vertical mainly within 3 months and the seedlings gradually shed leaves since late October which may further complicate the interpretation of RGSs.

Table 2 presents the experimental data calculated according to Huang's model. Spring-back strain (SBS) parameter (β) and RGS parameter (α) indicate the direction and the magnitude of gravitational force and gravitropic correction, respectively. The negative β value of all inclined seedlings indicates that the weight of the inclined trunk generated a downward bending moment. On the contrary, the negative α value indicates that the bending moment generated by tension wood was to pull the trunk upward. The magnitude of α within 3 months after inclination was the largest and it was larger at the trunk base (-508 ± 180 με) than at the half-height (-323 ± 256 με) ($t = -1.77$, $p < 0.05$, $n = 9$). The magnitude of α gradually reduced to near 0 and it was sooner at the half-height of the trunks than at the base (Fig. 10).

The mean RGS parameter (α) and the mean of eccentrically corrected RGS parameter (α') for 9 inclined seedlings (3 in the 2009 and 6 in the 2012 experiment) examined within 3 months after tilting were -418 με and -523 με, respectively. The promoted growth increment on the upper side of the inclined trunk increased the efficiency of correction by 25 %. Downward bending tendency was predicted in 9 out of 14 measuring sites in 10 inclined seedlings. The eccentric correction changed the downward bending tendency to upward at five measuring sites (Table 2).

The rate of curvature change due to self-weight (dC_s/dR) and negative gravitropism (dC_g/dR) were also shown in Table 2. In the 2009 experiment, the average dC_s/dR was -58.38 m^{-2} for seedlings examined 3 months after inclination and -31.12 m^{-2} for 6 month. In the 2012 experiment, dC_s/dR is -115.6 m^{-2} for the seedlings examined within 3 months. All dC_s/dR were negative, indicating a downward bending moment.

In the 2009 experiment, the average dC_g/dR was 69.09 for the inclined seedlings sampled 3 months after inclination and 30.01 m^{-2} for 6 months. In the 2012 experiment, dC_g/dR is 117.65 m^{-2} within 3 months after inclination. All dC_g/dR were positive except 1 site at the half-height in the 2009 experiment, indicating an upward bending moment. Corrected by eccentric radial growth, the mean rates of curvature change due to gravitropism (dC'_g/dR) increased to 136.89 and 66.73 m^{-2} for the seedlings sampled 3 and 6 months after inclination in the 2009 experiment and 127.2 m^{-2} in the 2012 experiment. The correction efficiency increased 98.1, 44.4 and 8.1 %, respectively.

The mean net rate of curvature change (dC/dR) is 10.72 and -1.11 m^{-2} for seedlings examined 3 and 6 months after inclination in the 2009 experiment, and 2.05 m^{-2} in the 2012 experiment. After corrected with asymmetric growth increment, the mean value of dC'/dR increased to 78.51, 12.23, and 11.6 m^{-2}, respectively.

Discussion

The stem mechanical properties and related anatomical features were often treated in separate scopes of researches; only few studies integrated them in a comprehensive study. As a reference of the branch, a documentation of trunk mechanical properties of *Koelreuteria henryi* is essential. In this paper, we attempt to understand the bending tendency of the inclined trunk of the seedlings, focusing on

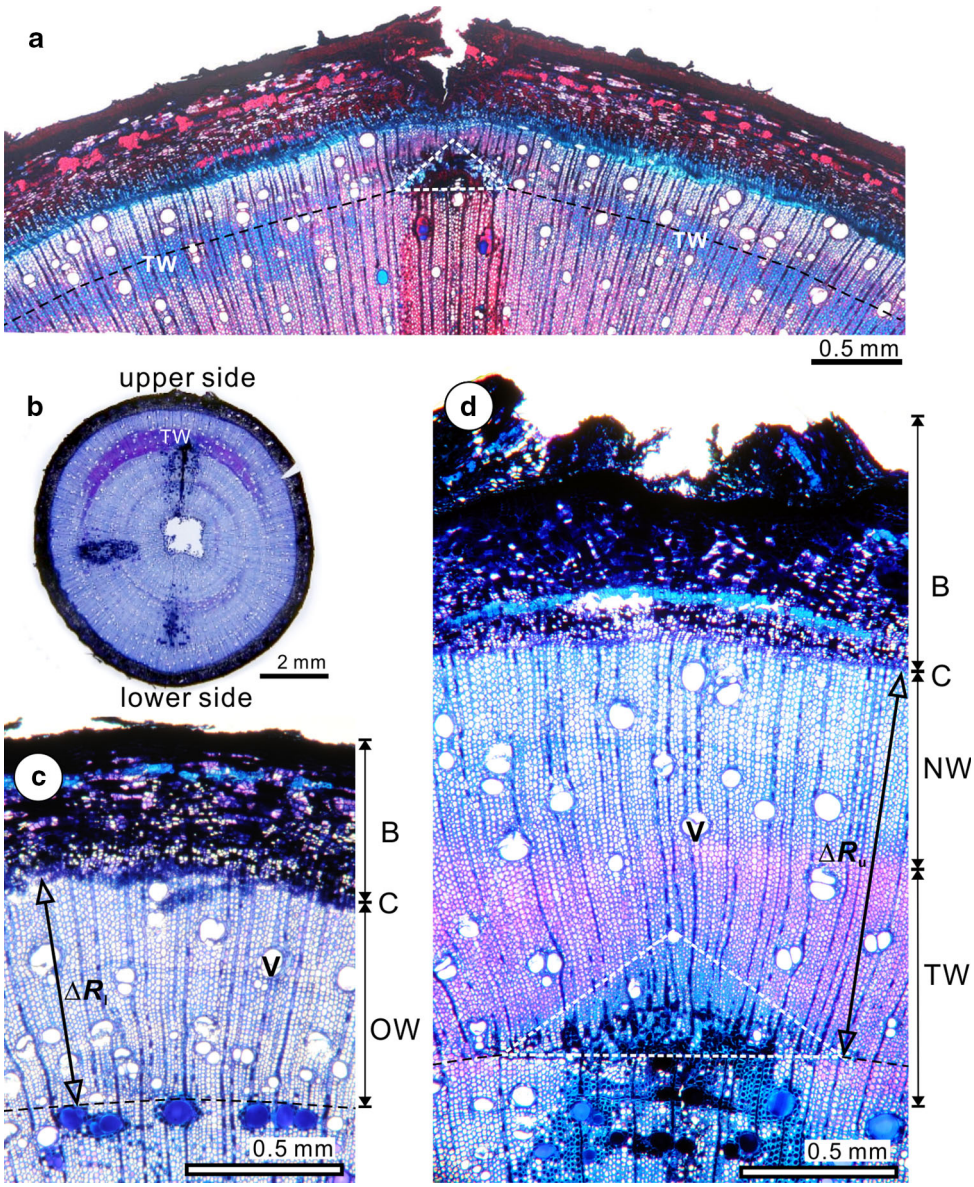

Fig. 7 Light micrographs of cross sections of the trunk of inclined *K. henryi* seedlings showing the tension wood formation. **a** The upper side at the trunk base of the T13 seedling collected after one-month inclination and the section was stained with safranin O and alcian blue. **b–d** Whole trunk section (**b**), the lower side part (**c**), and the upper side part (**d**) at the half-height of the trunk of the T4 seedling collected after six-months inclination and the section was stained with TBO. The triangular wound tissues induced by pinning (outlined by *white dotted lines* in **a**, **d**) directly marked the position of the vascular cambium at the onset of inclination (*blacked dotted lines* in **a**, **c**, **d**). Several layers of G-fibers were formed on the inner side of the marked cambial zone (**a**, **d**). Tension wood formed only on the upper side of the stem (**a**, **b**, **d**) but not in the lower side (**b**, **c**). *TW* tension wood, *B* bark, *C* cambium, *OW* opposite wood, *NW* normal wood, *V* vessel, ΔR_l *and* ΔR_u the wood growth increment on the lower and the upper side

both physical behavior and anatomical changes during the uprighting process of *K. henryi.*

Dynamics of the up-righting process of the inclined trunk

The reorientation of an inclined tree is based on asymmetric growth of the new axis created by the terminal bud at the primary growth level and of the pre-existing trunk at the secondary growth level (Thibaut et al. 2001). During the righting process the trunk curves upward continuously, while a counter autotropic curving initiated from the tip to keep the distal part of the trunk straight before reaching the vertical line (Moulia et al. 2006).

Koelreuteria henryi is a tropical deciduous tree with a growth season from March to December. By a whole year's observation (Fig. 2), we found the reorientation process of the inclined seedlings takes place mainly in the first 3 months after tilting. The gravitropic response of the tested inclined *K. henryi* seedlings is similar to that of young hybrid *Populus* studied by Coutand et al. (2007). They recognized three phases including the latent phase, the upward gravitropic phase, and the autotropic decurving phase during the righting process by analyzing the kinematics of curvature fields and tension wood distribution along the trunk. These phases were also recognized in *Pinus pinaster* by Sierra-De-Grado et al. (2008) and in 8 tropical angiosperm species by Alméras et al. (2009).

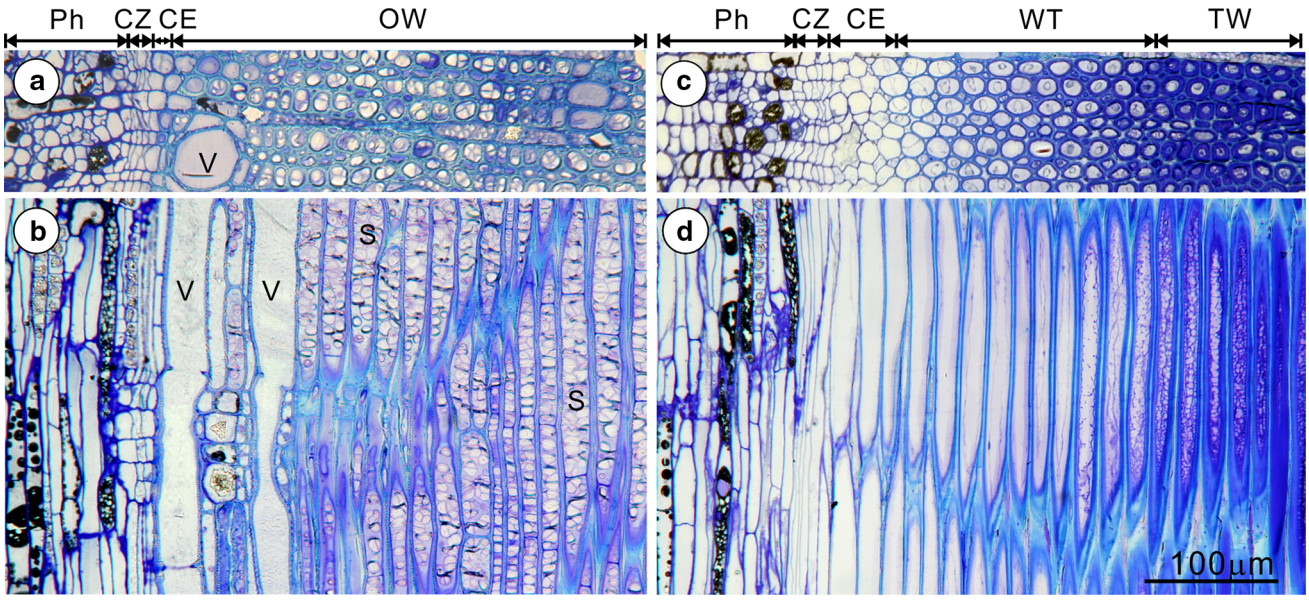

Fig. 8 Light micrographs of cross (**a**, **c**) and radial longitudinal (**b**, **d**) plastic sections of the lower (**a**, **b**) and the upper side (**c**, **d**) of the trunk of the T3 seedling. The cambial zone of the lower side is inactive and the opposite wood fibers were filled with starch grains (**a**, **b**). The cambial zone of the upper side was producing G-fibers. *Ph* phloem, *CZ* cambial zone, *CE* zone of cell enlargement, *WT* zone of cells under secondary wall thickening, *TW* tension wood with mature G-fibers, *OW* opposite wood, *V* vessel element, *S* starch grains

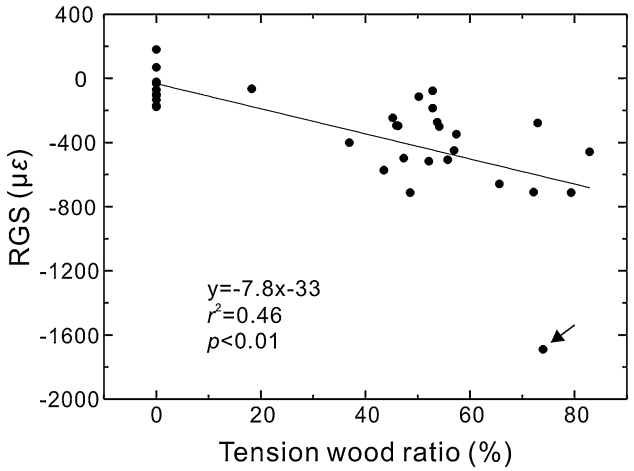

Fig. 9 The relationship between tension wood ratio and RGSs. The tension wood ratio was 0 % in control seedlings. RGSs were taken from the data of both sides of the 3 control seedlings sampled at July 23 2009 and the data of the upper side (ε_{gu}) of all 12 inclined seedlings in the 2009 experiment. *Arrow* indicates a potential outlier

Spatial and temporal RGSs distribution in the trunk of seedling

The intrinsic moving force generated by the wood structure of a tilted trunk is the cumulative effect of the stress on the upper side and on the lower side (Clair et al. 2006a; Huang et al. 2010). In general, typical RGS values for trunks range from −150 to −1000 με for normal wood, from −1000 to −4000 με for tension wood (Alméras et al. 2005; Clair et al. 2006a, c; Fournier et al. 1994b; Jullien et al. 2013; Kuo-Huang et al. 2007; Ruelle et al. 2007a). In seedlings, the magnitude of RGSs of tension wood is smaller (–600 to –1600 με) (Coutand et al. 2007; Coutand et al. 2014). Our results with *K. henryi* showed even lower RGSs in tension wood (−661.39 ± 351.10 με). Considering the seedling sizes in this study were smaller than those in the experiments of Coutand et al. (2014), our results support the trend that the smaller trees exhibit smaller levels of RGSs (Coutand et al. 2014). For *K. henryi* seedlings around 1 m in height, a relative small amount of tensile stress may be enough to pull the trunk back to an equivalent position, or the opposite wood may also contribute to the uprighting process.

In 21 angiosperm species been studied by Clair et al. (2006c), the RGS values on the upper side were 1.9 to 23.9 times of those on the lower side. The tensile stress on the upper side rather than the stress occurred on the lower side is considered to be the major source of upward bending moment (Clair et al. 2006b; Fang et al. 2008; Onaka 1949). However, in the opposite wood of angiosperm trees, both Kuo-Huang et al. (2007) and Clair et al. (2006a) observed some light compressive strains (+100 to +200 με). In *K. henryi* some stronger, positive compressive strains were also found. Furthermore, we noticed that the ability of a tree trunk to bend upward, expressed by RGS parameter (α), decreased during the uprighting process. This reduction of α is due to the decrease of RGSs on the lower side (ε_{gl}) (Fig. 10). We therefore propose that in seedlings of *K.*

Table 2 Experimental data of the inclined seedlings of *Koelreuteria henryi* for prediction of bending dynamics

Growth duration	Seedling	β (με)	α (με)	α′ (με)	β–α (με)	Bending tendency	β–α′	Bending tendency	dC_s/dR (m^{-2})	dC_g/dR (m^{-2})	dC/dR (m^{-2})	dC'_g/dR (m^{-2})	dC'/dR (m^{-2})
2009 experiment													
3 months	T1b	−331	−445	−595	114	UW	264	UW	−81.93	110.02	28.09	147.31	65.38
	T1h	−113	−91	−409	−22	DW	296	UW	−34.82	28.16	−6.65	126.46	91.64
Mean		−222	−268	−502	46		280		−58.38	69.09	10.72	136.89	78.51
6 months	T4b	−148	−99	−295	−49	DW	147	UW	−24.42	16.39	−8.03	48.84	24.42
	T4h	−92	9	−63	−101	DW	−29	DW	−23.44	−2.17	−25.60	15.95	−7.49
	T5b	−377	−356	−385	−22	DW	8	UW	−39.87	37.60	−2.27	40.69	0.82
	T5h	−112	−88	−97	−24	DW	−14	DW	−26.63	21.02	−5.61	23.20	−3.43
	T6b	−239	−371	−502	133	UW	263	UW	−35.25	54.83	19.58	74.13	38.88
	T6h	−145	−204	−223	60	UW	78	UW	−37.09	52.37	15.27	57.24	20.15
Mean		−185.50	−184.83	−260.83	−0.50		75.50		−31.12	30.01	−1.11	43.34	12.23
2012 experiment													
1 months	T13b	−790	−772	−739	−19	DW	−51	DW	−162.41	158.61	−3.80	151.88	−10.53
	T14b	−393	−477	−589	84	UW	197	UW	−108.18	131.34	23.15	162.35	54.16
2 months	T15b	−348	−334	−431	−14	DW	84	UW	−64.09	61.51	−2.58	79.56	15.47
	T16b	−746	−736	−847	−10	DW	101	UW	−128.63	126.90	−1.72	146.03	17.40
3 months	T17b	−670	−520	−582	−151	DW	−88	DW	−110.78	85.90	−24.88	96.26	−14.52
	T18b	−511	−605	−543	95	UW	33	UW	−119.51	141.64	22.12	127.15	7.63
Mean		−576.33	−574.00	−621.83	−2.50		46.00		−115.60	117.65	2.05	127.21	11.60

β spring-back strain parameter, α and α′ asymmetric released growth strain parameters, *DW* downward bending, *UW* upward bending, d*Cs*/d*R* rate of gravitational disturbance, d*Cg*/d*R* and d*C*′*g*/d*R* rates of gravitropic correction, d*C*/d*R* and d*C*′/d*R* net rates of curvature change

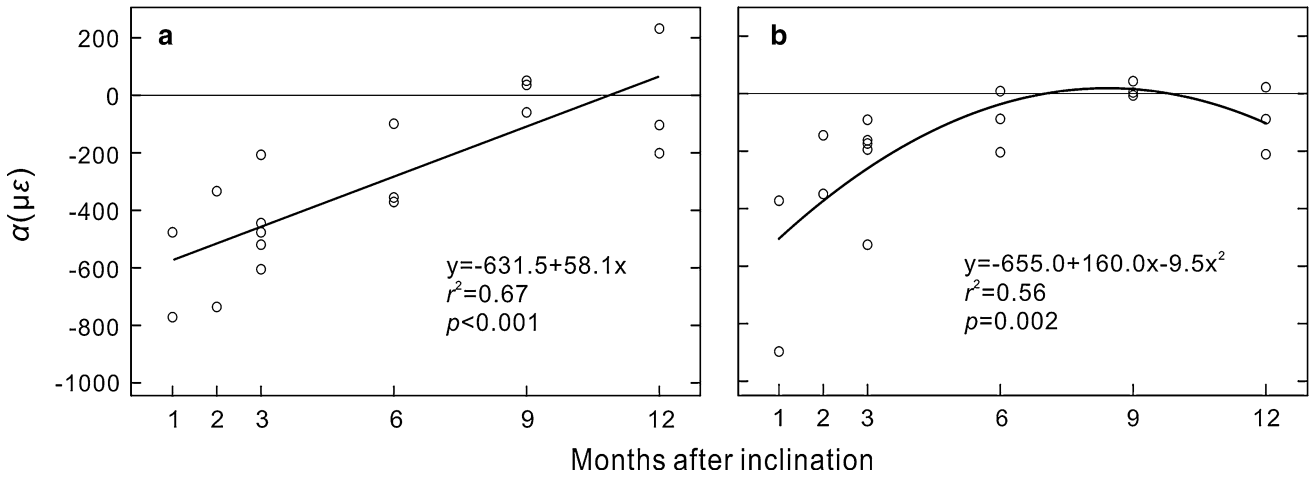

Fig. 10 Relationship of growth strain parameter (α) and inclination duration at the trunk base (**a**) and at the half-height (**b**). The magnitude of α was the largest in the first 3 months and gradually reduced to near 0

henryi, the tensile stress on the upper side and the compressive stress on the lower side work intimately to reorient the tilted trunks.

A spatial variation of RGS was found in the inclined seedlings of *Liriodendron tulipifera* and *Prunus spachiana*, the RGSs decreased with the tree height in both fixed and free parts of the trunks (Yoshida et al. 2000). Our experiment showed the same trend (Fig. 3), suggesting that the trunk base plays a key role in trunk reorientation. These results further explain the largest curvature found in the trunk base of poplar after 40 days of tilting (Coutand et al. 2007). The magnitude of α gradually reduced to near 0 and was sooner at the half-height of the trunks than at the base (Fig. 10).

Coutand et al. (2014) investigated the spatial and temporal variation in residual longitudinal maturation strains (rlms) weekly during the gravitropic response of young hybrid poplar. They found that the at 100 cm from the stem base the rlms reached the maximum at 35 days after tilting and then decreased; and the differential of rlms between upper and lower side changed from negative to positive at 47 days after tilting which indicating the beginning of the autotropic phase. In our study the RGS was measured monthly and at the stem we found that the magnitude of RGS on the upper side was large and lasted for 6 months (Fig. 3d); and the value of α had not reach 0 in 6 months (Fig. 10a). However, at the half-height the maximum RGS on the upper side was largest in 1 month after tilting and then decreased (Fig. 3c) which is similar to the observation of Coutand et al. (2014); and the value of α in one seedling reached 0 (Fig. 10b) indicating the beginning of the autotropic phase. These results suggest that the spatial and temporal variation in growth strain or stress are important in the study of gravitropic response.

Strain and tension wood ratio

Zinc chloride-iodine (Herzberg reagent) is commonly used to histochemically stain G-fibers in tension wood (Doğu and Grabner 2010; Grzeskowiak et al. 1996; Tsai et al. 2012). However, this dye stains also the starch a blackish color, seriously disturbing the measurement of tension wood zones. Both G-fibers and normal wood fibers of *K. henryi* are living fibers generally filled with starch grains. We therefore used zinc chloride-iodine to verify the presence of G-fibers, while resorting to the TBO staining in the delimitation and measurement of tension wood zones.

In *K. henryi*, the tension wood ratio is highly correlated to the RGSs (Fig. 9), which agrees with the previous studies (Fang et al. 2008; Okuyama et al. 1994; Washusen et al. 2003b). In 11-year-old *Eucalyptus globulus*, Washusen et al. (2003a) found that G-fibers presented in the investigated three populations at a level of −1200 με. In the non-conductive tissues of a leaning 15-year-old poplar tree, Fang et al. (2008) found no G-fibers under a growth strain level of −600 to −800 με, but 100 % G-fibers above a level of −1500 to −1900 με. In this study, the seedlings of *K. henryi* were younger and smaller than those in the previous studies. In all RGS measuring site on the upper side of inclined seedlings G-fibers were detected where the RGSs ranged from −64 to −712 με (with an outlier of −1690) (Fig. 9), which is smaller than the threshold listed above. We therefore propose that smaller trees produces tension wood with smaller growth strains. This hypothesis certainly needs to be verified with bigger dataset including more species and large span of seedling size.

The origin of G-fibers

We verify the origin of G-fibers with pinning method. Pinning method, first introduced by Wolter (1968), marks

the position of cambial zone at the time of pinning. This method is employed to monitor seasonal dynamics of cambial activity or wood formation for many tree species (Gričar et al. 2007; Mäkinen et al. 2008; Ohashi et al. 2001; Schmitt et al. 2004).

Concerning the research of reaction wood formation, Mukogawa et al. (2003) marked the vascular cambium with a knife instead of a pin to observe the eccentric growth of leaning trees in a macroscopic view. To study the phototropic and negative gravitropic bending, Matsuzaki et al. (2007) used pinning method to mark the radial direction and measured possible torsion of the main stem. We first employed the mothed to study the onset of artificially induced tension wood, and found it particularly useful in discriminating the origin of G-fibers induced by the inclining treatment without pre-experimental noise. Our results clearly showed that several developing fiber layers preceded pinning wound were turned into G-fibers (Fig. 7a, d), providing a direct evidence to support the proposal of Jourez and Avella-Shaw (2003) and Scurfield (1972). At the onset of tilting, the differentiating xylary fiber cells in different stages may react to gravitational stimulus and add a G-layer in the innermost cell wall. Thus, the cell wall may consist of layers P+S1+S2 +G, P+S1+G, or even P+S1+S2+S3+G. The quick transformation from developing cells to G-fibers allows the plant to promptly recover to an equivalence position. The formation of tension wood may result to the large contractive growth strain on the upper side (ε_{gu}) (Fig. 3), and finally bend the inclined seedlings to upright position. In our results, this recovering process lasted 3 months (Figs. 2, 3; Table 1). After the equilibrium has reached, the cells within vascular cambial region would then resume normal wood production.

The role of eccentric growth increment in gravitropic correction

Bending dynamics of a leaning trunk or a tilting branch depends on the mutual interaction of gravitational disturbance, phototropic response, and consequently the gravitropic correction (Alméras et al. 2005; Huang et al. 2010). Besides asymmetric growth strain and heterogeneous distribution of tension wood, the efficiency of gravitropic correction is also affected by eccentric growth increment. In the leaning trunk of a conifer, the additional radial growth is mostly found on the lower side, or hypotrophic. Despite some exceptions, the great majority of conifer branches are also hypotrophic with less pronounced eccentric growth than in trunks. Broadleaved trees are often epitrophic, i.e., additional growth on the upper side of leaning trunks, the branches of angiosperms were more complicated (Timell 1986). They were once regarded as epitrophic, however, a growing number of contradictions were published. In the branches of *Sassafras officinale*, tension wood formed on the upper side while growth promotion occurred on the lower side (White 1962). In species free of tension wood such as *Pseudowintera colorata* (Kuĉera and Philipson 1978) and *Viburnum odoratissimum* (Wang et al. 2009), growth increment was observed on the lower side. In a survey of eight angiosperm species with or without G-fibers, Tsai et al. (2012) found that the eccentricities are most positive (hypotrophic) in the branch base and generally decreased from basal to distal parts.

The eccentric growth in leaning trunks was found to increase the efficiency of reorientation by 31 % for angiosperms and 26 % for gymnosperms (Alméras et al. 2005). In this study, we found a 25 % increase in efficiency of correction in the inclined trunk of *K. henryi* seedlings and the reaction wood is associated with promoted growth increment. Formation of tension wood and eccentric radial growth were proposed to be driven by different mechanisms without functional relationship (Duncker and Spiecker 2008; Timell 1986); however, the co-occurrence of reaction wood and promoted growth increment at the same side in tree trunks is considered an "economic" solution to facilitate the reorientation process (Alméras et al. 2005).

Concerning the branches, eccentric growth increases efficiency of reorientation by 12.5 % in *Chamaecyparis formosensis* (gymnosperm) (Huang et al. 2010) and as in the trunk, the promoted radial growth was found on the same side of reaction wood. However, in the branches of *K. henryi*, the efficiency of reorientation decreases by 25 % in *K. henryi* (Huang et al. 2010), and the promoted growth occurs on the opposite side of reaction wood, probably causing the decrease of reorientation efficiency. It is interesting to find that the reaction wood formation in branches of *K. henryi* is not always on the upper side (Hung et al. unpublished data); therefore, the mechanism of branch reorientation of *K. henryi* awaits further investigation.

Conclusion

This work established the gravitropic reaction occurred in artificially inclined *Koelreuteria henryi* seedlings in both physical and anatomical respects. We confirmed that at the time of inclination both the developing fibers and the vascular cambium are able to perceive the signal of mechanical change and produce G-fibers that generate a strong contractile strain to pull the trunk upright until the equilibrium is reached. Stronger contractile RGS and more tension wood were found at the trunk base than at the half-height, suggesting that the trunk base plays a key role in trunk uprighting of *K. henryi* seedlings. The associated

eccentric growth increment has a 25 % increase in efficiency of correction with respect to the RGS parameter (α), that is, promote the upright movement. Since more variation between the wood structure and bending dynamics may occur in the branches, a study concerns the role of eccentric growth, tension distribution and the biomechanical features in branches of *K. henryi* with different angles is under progress.

Author contribution statement L.-F. Hung, C.-C. Tsai, and L.-L. Kuo-Huang designed the study. L.-F. Hung conducted the experiment, made the observation and measurement, performed the data analysis, and wrote the manuscript. C.-C. Tsai assisted with the measurement, data analysis, and manuscript preparation. S.-J. Chen provided the technical support and helped the data interpretation. L.-L. Kuo-Huang and Y.-S. Huang supervised the study and reviewed the drafts of the manuscript.

Acknowledgments The authors would like to thank Dr. Ching-Te Chien and Miss Chin-Mei Lee for technical support. This study was funded by the National Science Council, Taiwan through research project NSC-97-2313-B-002-043-MY3.

Compliance with ethical standards

Conflict of interest The authors declare that they have no conflict of interest.

References

Alméras T, Fournier M (2009) Biomechanical design and long-term stability of trees: morphological and wood traits involved in the balance between weight increase and the gravitropic reaction. J Theor Biol 256:370–381

Alméras T, Thibaut A, Gril J (2005) Effect of circumferential heterogeneity of wood maturation strain, modulus of elasticity and radial growth on the regulation of stem orientation in trees. Trees 19(4):457–467

Alméras T, Derycke M, Jaouen G, Beauchene J, Fournier M (2009) Functional diversity in gravitropic reaction among tropical seedlings in relation to ecological and developmental traits. J Exp Bot 60(15):4397–4410

Archer RR (1986) Growth stresses and strains in tress. Springer, Berlin

Baba K, Park YW, Kaku T, Kaida R, Takeuchi M, Yoshida M, Hosoo Y, Ojio Y, Okuyama T, Taniguchi T, Ohmiya Y, Kondo T, Shani Z, Shoseyov O, Awano T, Serada S, Norioka N, Norioka S, Hayashi T (2009) Xyloglucan for generating tensile stress to bend tree stem. Mol Plant 2(5):893–903

Batianoff GN, Butler DW (2002) Assessment of invasive naturalised plants in south-east Queensland. Plant Prot Q 17:27–34

Clair B, Alméras T, Pilate G, Jullien D, Sugiyama J, Riekel C (2011) Maturation stress generation in poplar tension wood studied by synchrotron radiation microdiffraction. Plant Physiol 155(1):562–570

Clair B, Alméras T, Sugiyama J (2006a) Compression stress in opposite wood of angiosperms: observations in chestnut, mani and poplar. Ann For Sci 63(5):507–510

Clair B, Alméras T, Yamamoto H, Okuyama T, Sugiyama J (2006b) Mechanical behavior of cellulose microfibrils in tension wood, in relation with maturation stress generation. Biophys J 91(3):1128–1135

Clair B, Ruelle J, Beauchéne J, Prévost MF, Fournier M (2006c) Tension wood and opposite wood in 21 tropical rain forest species 1. Occurrence and efficiency of the G-layer. IAWA 27(3):329–338

Coutand C, Fournier M, Moulia B (2007) The gravitropic response of poplar trunks: Key roles of prestressed wood regulation and the relative kinetics of cambial growth versus wood maturation. Plant Physiol 144(2):1166–1180

Coutand C, Pot G, Badel E (2014) Mechanosensing is involved in the regulation of autostress levels in tension wood. Trees 28(3):687–697

Doğu AD, Grabner M (2010) A staining method for determining severity of tension wood. Turk J Agric For 34(5):381–392

Donaldson L (2008) Microfibril angle: measurement, variation and relationships—a review. IAWA 29(4):345–386

Duncker P, Spiecker H (2008) Cross-sectional compression wood distribution and its relation to eccentric radial growth in *Picea abies* [L.] Karst. Dendrochronologia 26(3):195–202

Ewart AJ, Mason-Jones AJ (1906) The formation of red wood in conifers. Ann Bot 20:201–204

Fang CH, Clair B, Gril J, Alméras T (2007) Transverse shrinkage in G-fibers as a function of cell wall layering and growth strain. Wood Sci Technol 41:659–671

Fang CH, Clair B, Gril J, Liu SQ (2008) Growth stresses are highly controlled by the amount of G-layer in poplar tension wood. IAWA 29(3):237–246

Fisher JB, Stevenson JW (1981) Occurrence of reaction wood in branches of dicotyledons and its role in tree architecture. Bot Gaz 142(1):82–95

Fournier M, Bailleres H, Chanson B (1994a) Tree biomechanics: growth, cumulative prestresses, and reorientations. Biomimetics 2(3):229–251

Fournier M, Chanson B, Thibaut B, Guitard D (1994b) Measurements of residual growth strains at the stem surface. Ann For Sci 51(3):249–266

Gardiner B, Barnett J, Saranpää P, Gril J (2014) The biology of reaction wood. Springer, Berlin, p 274

Gričar J, Zupančič M, Čufar K, Oven P (2007) Wood formation in Norway spruce (*Picea abies*) studied by pinning and intact tissue sampling method. Wood Res 52(2):1–9

Grzeskowiak V, Sassus F, Fournier M (1996) Macroscopic staining, longitudinal shrinkage and growth strains of tension wood of poplar (*Populus* × *euramericana* cv I.214). Ann Sci For 53(6):1083–1097

Höster HR, Liese W (1966) On the occurrence of reaction tissue in roots and branches of dictyledons. Holzforschung 20:80–90

Huang YS, Hung LF, Kuo-Huang LL (2010) Biomechanical modeling of gravitropic response of branches: roles of asymmetric periphery growth strain versus self-weight bending effect. Trees 24(6):1151–1161

Jourez B, Avella-Shaw T (2003) Effet de la durée d'application d'un stimulus gravitationnel sur la formation de bois de tension et de bois opposé dans de jeunes pousses de peuplier (*Populus euramericana* cv 'Ghoy'). Ann For Sci 60:31–41

Jullien D, Widmann R, Loup C, Thibaut B (2013) Relationship between tree morphology and growth stress in mature European beech stands. Ann For Sci 70(2):133–142

Kuĉera LJ, Philipson WR (1978) Growth eccentricity and reaction anatomy in branchwood of *Pseudowintera colorata*. Am J Bot 65(6):601–607

Kuo-Huang LL, Chen SS, Huang YS, Chen SJ, Hsieh YI (2007) Growth strains and related wood structures in the leaning trunks and branches of *Trochodendron aralioides*—a vessel-less dicotyledon. IAWA 28(2):211–222

Mäkinen H, Seo JW, Nöjd P, Schmitt U, Jalkanen R (2008) Seasonal dynamics of wood formation: a comparison between pinning,

microcoring and dendrometer measurements. Eur J For Res 127(3):235–245
Matsuzaki J, Masumori M, Tange T (2007) Phototropic bending of non-elongating and radially growing woody stems results from asymmetrical xylem formation. Plant Cell Environ 30(5):646–653
Mellerowicz EJ, Gorshkova TA (2012) Tensional stress generation in gelatinous fibres: a review and possible mechanism based on cell-wall structure and composition. J Exp Bot 63(2):551–565
Mellerowicz EJ, Immerzeel P, Hayashi T (2008) Xyloglucan: the molecular muscle of trees. Ann Bot 102(5):659–665
Moulia B, Coutand C, Lenne C (2006) Posture control and skeletal mechanical acclimation in terrestrial plants: implications for mechanical modeling of plant architecture. Am J Bot 93(10):1477–1489
Mukogawa Y, Nobuchi T, Sahri MJ (2003) Tension wood anatomy in artificially induced leaning stems of some tropical trees. For Res 75:27–33
Nishikubo N, Takahashi J, Roos AA, Derba-Maceluch M, Piens K, Brumer H, Teeri TT, Stalbrand H, Mellerowicz EJ (2011) Xyloglucan *endo*-transglycosylase-mediated xyloglucan rearrangements in developing wood of hybrid aspen. Plant Physiol 155(1):399–413
Ohashi Y, Sahri MH, Yoshizawa N, Itoh T (2001) Annual rhythm of xylem growth in rubberwood (*Hevea brasiliensis*) trees grown in Malaysia. Holzforschung 55(2):151–154
Okuyama T, Yamamoto H, Yoshida M, Hattori Y, Archer RR (1994) Growth stresses in tension wood—role of microfibrils and lignification. Ann Sci For 51(3):291–300
Onaka F (1949) Studies on compression- and tension-wood. Mokuzai Gakkaishi 1:1–88
R Core Team (2013) R: a language and environment for statistical computing
Ruelle J, Beauchene J, Yamamoto H, Thibaut B (2011) Variations in physical and mechanical properties between tension and opposite wood from three tropical rainforest species. Wood Sci Technol 45(2):339–357
Ruelle J, Yamamoto H, Thibaut B (2007a) Growth stresses and cellulose structural parameters in tension and normal wood from three tropical rainforest angiosperms species. Bioresources 2(2):235–251
Ruelle J, Yoshida M, Clair B, Thibaut B (2007b) Peculiar tension wood structure in *Laetia procera* (Poepp.) Eichl. (Flacourtiaceae). Trees 21(3):345–355
Schmitt U, Jalkanen R, Eckstein D (2004) Cambium dynamics of *Pinus sylvestris* and *Betula* spp. in the northern boreal forest in Finland. Silva Fenn 38(2):167–178
Scurfield G (1972) Histochemistry of reaction wood cell walls in two species of *Eucalyptus* and in *Tristania conferta* R. BR. Aust J Bot 20:9–26
Scurfield G (1973) Reaction wood: its structure and function: lignification may generate the force active in restoring the trunks of leaning trees to the vertical. Science 179(4074):647–655
Sierra-De-Grado R, Pando V, Martinez-Zurimendi P, Penalvo A, Bascones E, Moulia B (2008) Biomechanical differences in the stem straightening process among *Pinus pinaster* provenances. A new approach for early selection of stem straightness. Tree Physiol 28(6):835–846
Sinnott EW (1952) Reaction wood and the regulation of tree Form. Am J Bot 39(1):69–78
Spurr A (1969) A low-viscosity epoxy resin embedding medium for electron microscopy. J Ultrastruct Res 26:31–43
Thibaut B, Grila J, Fournier M (2001) Mechanics of wood and trees: some new highlights for an old story. C R Acad Sci Paris Série II b 329(9):701–716
Timell TE (1986) Compression wood in gymnosperms, vol 2. Springer, Berlin, pp 748–754, 861–864
Tsai CC, Hung LF, Chien CT, Chen SJ, Huang YS, Kuo-Huang LL (2012) Biomechanical features of eccentric cambial growth and reaction wood formation in broadleaf tree branches. Trees 26(5):1585–1595
Wang Y, Gril J, Sugiyama J (2009) Variation in xylem formation of *Viburnum odoratissimum* var. *awabuki*: growth strain and related anatomical features of branches exhibiting unusual eccentric growth. Tree Physiol 29(5):707–713
Wardrop AB, Dadswell HE (1948) The nature of reaction wood. I. The sturcture and properties of tension wood fibres. Aust J Sci Res 1:1–16
Wardrop AB, Dadswell HE (1950) The nature of reaction wood II. The cell wall organization of compression wood tracheids. Aust. J Biol Sci 3(1):1–13
Wardrop AB, Dadswell HE (1955) The nature of reaction wood. IV. Variations in cell wall organization of tension wood fibres. Aust J Bot 3(2):177–189
Washusen R, Ilic J, Waugh G (2003a) The relationship between longitudinal growth strain and the occurrence of gelatinous fibers in 10 and 11-year-old *Eucalyptus globulus* Labill. Holz Roh Werkst 61(4):299–303
Washusen R, Ilic J, Waugh G (2003b) The relationship between longitudinal growth strain, tree form and tension wood at the stem periphery of ten- to eleven-year-old *Eucalyptus globulus* Labill. Holzforschung 57(3):308–316
White DJB (1962) Tension wood in a branch of sassafras. J I Wood Sci 10:74–80
Wilson BF, Archer RR (1977) Reaction wood—induction and mechanical action. Annu Rev Plant Phys 28:23–43
Wilson BF, Archer RR (1979) Tree design: some biological solutions to mechanical problems. Bioscience 29(5):293–298
Wolter KE (1968) A new method for marking xylem growth. For Sci 14(1):102–104
Yoshida M, Okuda T, Okuyama T (2000) Tension wood and growth stress induced by artificial inclination in *Liriodendron tulipifera* Linn. and *Prunus spachiana* Kitamura f. ascendens Kitamura. Ann For Sci 57(8):739–746
Yoshimura K, Hayshi S, Itoh T (1981) Studies on the improvement of the pinning method for marking xylem growth I. Minute examination of pin marks in taeda pine and other species. Wood Res 67:1–16
Yoshizawa N, Satoh M, Yokota S, Idei T (1993a) Formation and structure of reaction wood in *Buxus microphylla* var. *insularis* Nakai. Wood Sci Technol 27:1–10
Yoshizawa N, Watanabe N, Yokota S, Idei T (1993b) Distribution of guaiacyl and syringyl lignins in normal and compression wood of *Buxus microphylla* var. *insularis* Nakai. IAWA 14(2):139–151